http://dx.doi.org/10.21611/qirt.2006.022

Thermal transient mapping systems for integrated semiconductor devices and circuits.

Lucio Rossi*, Giovanni Breglio*, Andrea Irace*, Paolo Spirito*

*Università degli Studi di Napoli Federico II,Dipartimento di Ingegneria Elettronica e delle Telecomunicazioni, via Claudio 21, 80125 Napoli

Abstract

Aim of this paper is to present two systems for the acquisition of dynamic thermal maps of ICs, developed at the University of Naples "Federico II", Department of Electronic Engineering and Telecommunication (DIET). First of the two is a system that measures the infrared radiation emitted by a device or an electronic system undergoing a periodic electro-thermal transient, with a time resolution in the order of 2 μs and a temperature resolution in the order of 100 mK. The second system exploits the thermo-optic effect to measure the superficial temperature with a time resolution in the order of tenths of nanosecond and a temperature resolution of some Kelvin, along with a much better spatial resolution with respect to the other.

1. Introduction

The interaction between thermal and electrical parameters can lead to positive feedback effects that can cause malfunction or even instability and damage in electronic devices. This is the reason why modern power devices design is getting more and more concerned about the electro thermal dynamics of integrated devices and circuits. Besides this, modern day power devices and integrated circuits are getting always faster and smaller causing the electro-thermal phenomena to be much more difficult to follow in time and very localized in space. This is the reason why commercial FPA which are somewhat limited in their spatial and time resolution must be substituted by a single sensor approach. This means that the acquisition have to be repeated a several number of times focusing different spots of the device surface if we aim to retrieve a full map of temperature, but it's the price to be paid in order to achieve the demanding performances of ICs thermal imaging.

Speaking about methods of investigation, many have been exploited for this purpose, each one with its peculiar features and benefits. A concise description of the most common thermal imaging techniques is given in the following.

1.1. Liquid Crystals

Some cholesteric materials exhibit, when heated, a mesomorphic state with peculiar optic characteristics especially if deposited in thin layers. The change in colour of these materials can be related to the temperature variation on the surface of an electronic device. This is a very simple and cheap technique that can give good temperature and spatial resolutions but it is inherently slow and, being absolutely not contactless, it alters the boundary conditions of the thermal phenomenon.

http://dx.doi.org/10.21611/qirt.2006.022

1.2. AFM

Atomic Force Microscopy while being far more expensive than the latter technique is definitely the one that gives the best performances in terms of temperature and spatial resolution. A micromachined probe tip with a thermocouple is suspended by means of a cantilever on top of the DUT surface. A piezoelectric actuator is used to keep the atomic forces between the surface and the tip steady. The voltage needed to achieve this goal is related to the superficial topography while the thermocouple tip gives the temperature information.

1.3. Infrared technique

Any material at a temperature above 0 K emits in the infrared spectrum. If the emissivity coefficient on the DUT surface is accurately known it is possible to relate the emission in the infrared spectrum to the temperature. This technique shows optimum features of time and temperature resolution and a good spatial resolving power even though inherently limited by the infrared wavelength.

1.4. Thermoreflectance technique

Any change in temperature determines a change in the refractive index of a material. This obviously alters its reflectivity and so any change in the intensity of the light reflected by the DUT surface can be in principle related to the temperature variation. As in the case of the IR thermography the coefficient that links temperature and reflectivity must be properly measured first. As we are going to show in the following this approach can give a better resolution in terms of space and time respectively but remains limited in temperature sensitivity.

2. Infrared mapping system

As already pointed out before, the physical phenomenon that stands at the base of this technique is the emission of a hot body in the infrared radiation spectrum. Before going into further details, let's consider Plank's law which gives the power emitted by black body, defined as the perfect absorber (and emitter) at a specific wavelength in the IR spectrum:

$$W_t = \frac{2c^2 h}{\lambda^5 \left(e^{\frac{hc}{k\lambda T}} - 1 \right)} \qquad (2.1)$$

For any other material W should be multiplied by a coefficient known as emissivity which in general is dependent on the wavelength of emission and on temperature too.

Along with the power emitted by the body, part of the infrared power that comes from the surroundings is either reflected by or transmitted through the sample.

The total radiating power that comes to the sensor can be written as:

$$W_O = \varepsilon W_t + \rho W_{rb} + \tau W_{rb} \qquad (2.2)$$

http://dx.doi.org/10.21611/qirt.2006.022

Where W_t is the IR power emitted by a black body at the same temperature and W_{rb} is the ambient radiation, while ρ and τ are the reflectance and transmittance respectively. If we consider a body at thermal equilibrium then:

$$\varepsilon = \alpha$$

Where α is the absorbance. Besides that, the Kirchoff law relates all the above coefficients:

$$\alpha + \rho + \tau = 1 \tag{2.3}$$

It must be pointed out here that the value of the emissivity coefficient is not uniform on top of the DUT which means that in order to obtain a thermal map that is not emissivity affected we should measure its value point-by-point. This can be carried out easily under some assumptions.

Consider an opaque, grey body with an emissivity not dependent on temperature, and that the dependency between the signal detected and temperature, for a limited temperature swing, is linear. Then if we acquire a thermal map at ambient temperature and another at $T_{amb}+\Delta T$ we can write:

$$S_{\Delta T}(x,y) = S_{amb}(x,y) + \frac{\varepsilon(x,y)}{c}\Delta T \tag{2.4}$$

Which expresses the signal acquired at a temperature $T_{amb}+\Delta T$ as the sum of the signal acquired at T_{amb} temperature and a term which depends linearly on the temperature variation via the emissivity and the scaling factor c.

In any other case if the signal at the sensor is written as $S(x,y)$, the temperature on each point of the DUT surface can be calculated as:

$$\begin{aligned} T(x,y) &= T_{amb} + \frac{c}{\varepsilon(x,y)}\left(S(x,y) - S_{amb}(x,y)\right) \\ &= T_{amb} + \Delta T\,\frac{S(x,y) - S_{amb}(x,y)}{S_{\Delta T}(x,y) - S_{amb}(x,y)} \end{aligned} \tag{2.5}$$

Where ε and c finally cancel out.

2.1. The Optical chain

In Fig. 1 an outline of the radiometry system is shown. Starting from the bottom of the chain the DUT is moved under the microscope lens thanks to two translational stages (Physic Intrumente M-155.11) with a 0.1 μm resolution. Under the device a PID (Eurotherm 2416) controlled heating-cooling system with two Peltier cells is provided to set the temperature of the sample and acquire the emissivity map.

The radiation emitted by the DUT and the light reflected in the visible range after entering the microscope objective, are separated by a hot mirror.

The visible channel ends up with a CCD camera (Waitec) having a 10x magnification coefficient which is used to give visual information on the position and focusing of the microscope.

http://dx.doi.org/10.21611/qirt.2006.022

At the end of the IR channel J15TE (Judson) infrared detector working in the MIR range (2-5 μm) at a temperature of -80 °C. The temperature of the detector is kept steady by a TC5 controller (Judson) thanks to a three stages Peltier cell.

Since this sensor is a low impedance device a low noise preamplifier (PA101) is needed to retrieve the signal.

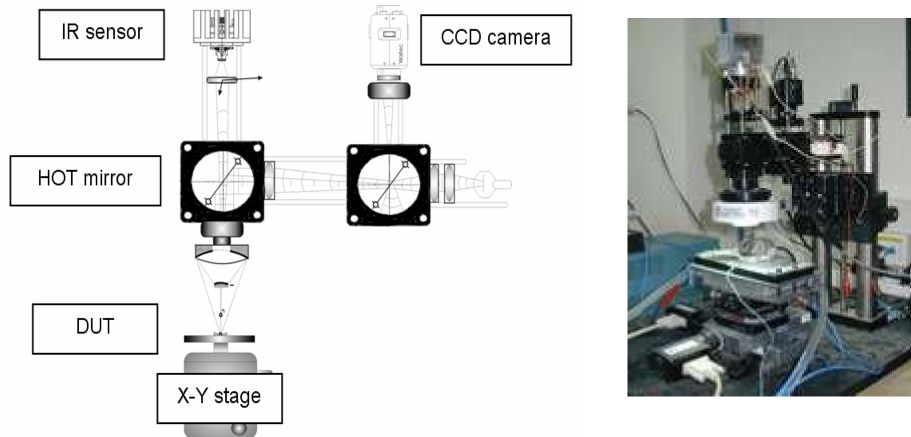

Fig.1 *Optical chain of the IR thermal mapping system*

Each and every one of the instruments that make up the system are controlled under a Matlab environment.

2.2. Features

Tab.1 *IR microscope main features.*

Spatial resolution	Thermal resolution	Thermal range	Time resolution	Invasivity	Complexity and cost
10 μm	0.1K	Tamb-500°C	1.5 μs	no	Medium-low

Starting from the spatial resolution, in the IR system the main limit is due to diffractive effects. According to the Sparrow criterion in fact the spatial resolution is related to the numerical aperture of the microscope objective by the following equation:

$$r = \frac{0.61\lambda}{NA} \tag{2.6}$$

Since the numerical aperture of the objectives used to magnify the DUT is in the order of 0.5, the resolution results close to the radiation wavelength. This is of

http://dx.doi.org/10.21611/qirt.2006.022

course an intrinsic limit of the IR approach, but since the optic window detected by the Judson sensor is the MIR (2-5 μm), resolutions of about 10 μm can be achieved anyway.

The detector's preamplifier PA101 is the device that sets the time limit of the whole system. For noise reasons, its bandwidth is limited to 1 MHz, which means that transients in the order of 1 μs can be followed.

To calculate the temperature resolution of the system let's consider first of all the power per unit wavelength coming to the detector:

$$P_{\lambda} = \tau_{\lambda} N_{\lambda} \Gamma \tag{2.7}$$

Where N_{λ} is the spectral power density emitted by the target, τ_{λ} is a transmission coefficient that takes into account the effect of all the elements in the chain while Γ is the reflection coefficient of the detector surface.

This has to be multiplied by the responsivity function of the sensor and then integrated over the entire wavelength window:

$$V_{out}(T) = A_{PA} \Gamma \int_{\lambda_1}^{\lambda_2} \tau(\lambda) N(\lambda, T) s(\lambda) d\lambda \tag{2.8}$$

Where the term A_{PA} is the amplification of the preamplifier. Taking the derivative of Eq. (2.8) versus temperature, it is possible to calculate the minimum temperature resolution of the whole system:

$$\Delta T_{\min} = \frac{\Delta v_{\min}}{k \int_{\lambda_1}^{\lambda_2} \tau(\lambda) \frac{\partial N(\lambda, T)}{\partial T} s(\lambda) d\lambda} \tag{2.9}$$

Which for a minimum detectable voltage of 0.1 mV for example gives the temperature resolution graph showed in Fig. 2.

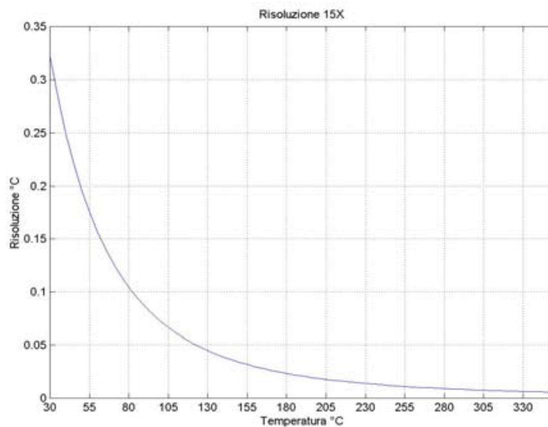

Fig.2 *Temperature resolution of the IR microscope*

http://dx.doi.org/10.21611/qirt.2006.022

2.3. Measurements

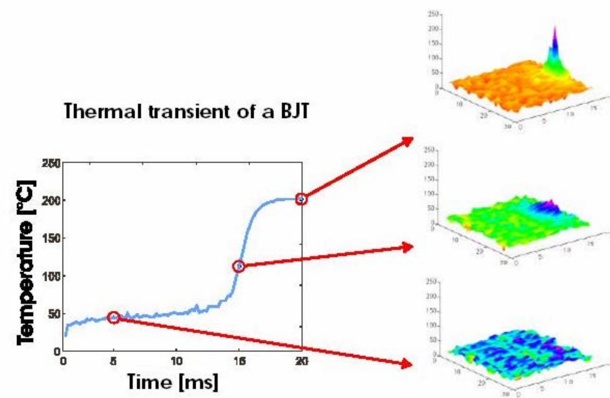

Fig.3 *Thermal transient of a BJT*

Many devices and in many different biasing configurations have been measured with this apparatus. One example is given in Fig. 3 where a 5x5 mm area of a switching BJT has been temperature mapped. The spacing of the grid used was around 50 μm to have a faster acquisition even if the system is capable of much higher spatial resolutions. Current flowing was in the order of some Amps over a 20 ms transient.

3. Thermoreflectance mapping system

This system is based on a single point sensor which measures the variation of the reflection coefficient due to a temperature change in metals and semiconductors. Being no longer limited to the IR spectrum this system is less limited by diffractive effects (see Eq. (2.6)) which grants an improved spatial resolution and also, since the reflection coefficient variation is very fast and modern photodiodes have bandwidths in excess of 1 GHz even time resolution can be improved.

To understand the physics underneath the thermoreflectance technique, consider for example the case of a simple interface between metal and air. The reflection coefficient can be expressed as follows:

$$R = \left| \frac{n_{air} - \tilde{n}_{met}}{n_{air} + \tilde{n}_{met}} \right|^2 \tag{3.1}$$

Where the refractive indexes of the two mediums are represented by the following equations:

$$\begin{aligned} &\tilde{n}_{met}(T) = n_{met} + jk_{met} \\ &n_{air \simeq 1} \end{aligned} \tag{3.2}$$

http://dx.doi.org/10.21611/qirt.2006.022

The real and imaginary part of the complex index of the metal are both temperature dependant. This dependency is influenced by a number of factors. First of all the material, in fact there is a big difference between the behaviour of metals compared to semiconductors which usually exhibit a much stronger dependence of the refractive index vs. temperature. Besides this the wavelength, but also the degree of superficial finishing and the specific technology used to grow a layer of material have some level of thermo optic influence.

Since the surface of an integrated device or system is usually made up of a wide variety of materials, the problem of determining a point-wise relationship between temperature and reflection coefficient arises.

To achive this goal we decided to perform a measurement of the so called thermoreflectance coefficient during data acquisition and for each and every point of the DUT. This coefficient relates the relative reflectance change to the temperature variation through the following equation:

$$\frac{\Delta R\left(T(t)\right)}{R}=\left[\frac{1}{R}\frac{\partial R}{\partial T}\right]\Delta T(t)=k_{TR}\Delta T \tag{3.3}$$

In order to obtain a point-wise measurement of this parameter we heated up the DUT at two different temperatures and measured the variation in the reflected light obtaining a complete 2D k_{TR}-matrix.

Typical values of the k coefficient for aluminium and silicon are given below:

$$\begin{aligned} k_{Al} &= (2.55\pm 0.15)10^{-5}K^{-1} \\ k_{Si} &= 1.5\cdot 10^{-4}K^{-1} \end{aligned} \tag{3.4}$$

Since this coefficient is not very high for aluminium as for the majority of metals, the main limit of the system will be the temperature resolution on areas covered by such materials.

3.1. The Optical Chain

A 660 nm, 10 mW (Miniature Fiber-Coupled diode Laser Melles-Griot) laser is 50% split for input power probing purposes by a first beam splitter and then split again by a second one which is used to separate incident and reflected light. The light is then focused on top of the DUT by a 20x microscope lens (Mitutoyo) with a 10 mm focal length and a resolving power of 0.7 µm. After being reflected on the device surface it goes back on the optical chain and is probed by a high-speed silicon photodetector (DET210 Thorlabs). It is worth notice that the beam splitters are inserted in a complementary configuration in order to compensate for the beam deviation.

A Peltier cell along with a running water heat sink serves the purpose of heating-cooling the device and bring it to a precise uniform temperature measured by a small thermocouple. Once the temperature is precisely set, thanks to a Eurotherm 2216a temperature controller, the intensity of light at the photodiode is measured and data is stored. In this way the thermoreflectance coefficient can be calculated point by point.

http://dx.doi.org/10.21611/qirt.2006.022

Two stepper motors with a 0.1 μm resolution (M-410 CG Physik Instrumente) are used to move the DUT underneath the laser focus to cover the area of interest.

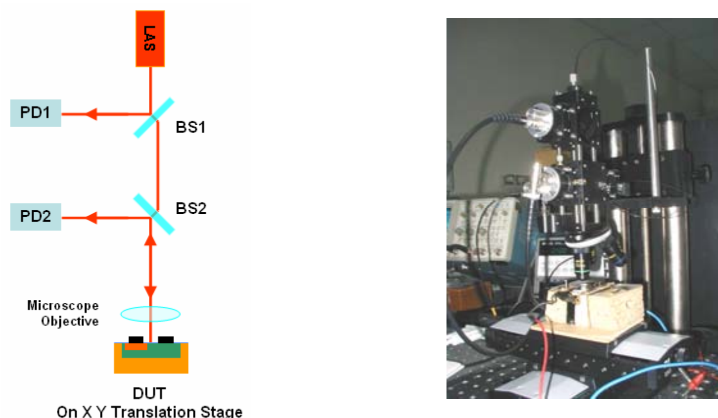

Fig.4 *Thermoreflectance system optical chain*

As in the case of the IR microscope all the instruments belonging to the system are controlled in a Matlab environment.

3.2. Features

Table 2. *Thermoreflectance imaging system features*

Spatial resolution	Thermal resolution	Thermal range	Time resolution	Invasivity	Complexity and cost
sub μm	3 K	0-350°C	Less than 10ns	no	Medium-low

Again the spatial resolution can be derived by Eq. (2.6) and (as taken from the data sheet of the microscope objective) at the wavelength of interest (660 nm) it is around 0.7 μm.

The time resolution of the whole system is limited by the photodiode bandwidth only. Considering the formula that relates the upper frequency limit to the junction capacitance and the load resistance:

$$f_{BW} = \frac{1}{2\pi R_L C_j} \qquad (3.5)$$

If R_L is 50 Ω (low sensitivity configuration) the upper bandwidth limit is greater than 1 GHz.

To calculate the thermal resolution considering that the temperature variation is proportional to the voltage variation at the photodiode we can write:

http://dx.doi.org/10.21611/qirt.2006.022

$$\delta T = \frac{\delta V}{k_{TR}} = \frac{R(\lambda) * R_L * \delta P}{k_{TR}} \tag{3.6}$$

Where $R(\lambda)$ is the responsivity of the photodiode and R_{LOAD} is the impedance of the load which, to achieve a higher sensitivity, is usually chosen as 1 MΩ.

If the input power is equal to the total noise power the terms written in the above equation represent the theoretical thermal resolution of the system, which for the case of silicon and considering the noise of the detector (shot and quantum) and the contribution of the load (Johnson) as uncorrelated sources, results:

$$\delta T = \frac{R_L}{k_{Si}} \sqrt{i_n^2 + i_{Johnson}^2} = 2.79°C \tag{3.7}$$

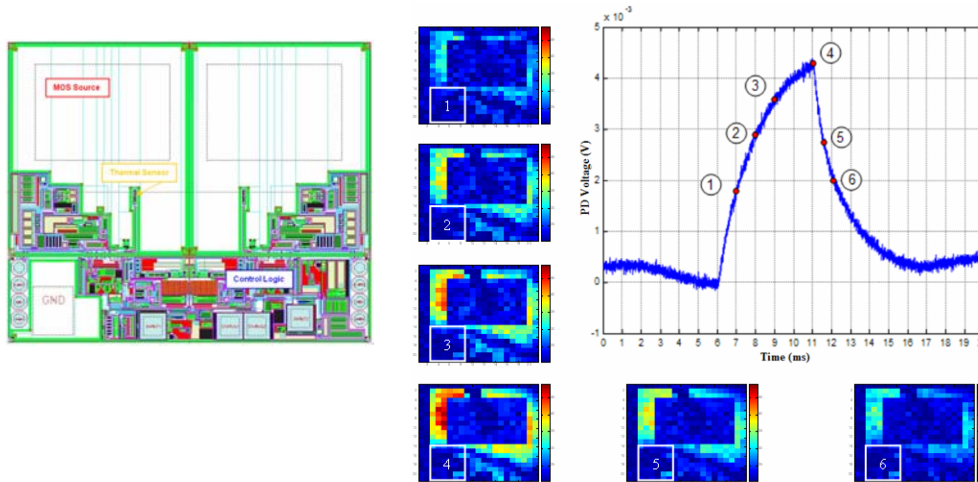

***Fig. 5** Layout and thermal transient of a VND810PEP power MOS device*

3.3. Measurements

A power MOS device has been used to analyze the performances of the system. In Fig.5 the layout of the VND810PEP is showed. This is a power MOS designed by ST-Microelectronics that exploits the VIPower technology. The source area of the device should be crossed by a uniform distribution of the current which in this technology flows vertically. The source, apart from the contact pad, is uniformly covered by silicon nitride so a large area has the same thermoreflectance coefficient.

Some still frames of the device thermal mapping are showed in Fig.5, where a large area shielded by the contact pad and the wiring is still visible. A 5 ms current pulse was used to heat up the device. During the on-time a 2 A current was flowing across the power MOS which reached a maximum temperature of about 50 °C (see Fig.5 frame 4).

The maps showed in this figure cover a 2000x2000 μm^2 wide area at a resolution of 100 μm which is far bigger than the intrinsic resolution limit of the system but

http://dx.doi.org/10.21611/qirt.2006.022

enough to give a fairly good description of the device behaviour without suffering the cost of a too long measurement time.

REFERENCES

[1] G. Breglio, P. Spirito, "Experimental detection of time dependent temperature maps in power bipolar transistors", MicroElectronic Journal, vol.31/9-10, pp. 735-739, 2000

[2] G. Breglio, N. Rinaldi, P. Spirito, "Thermal Mapping and 3D Numerical Simulation of New Cellular Power MOS Affected by Electro-Thermal Instability", MicroElectronic Journal, vol. 31/9-10, pp. 741-746, 2000

[3] D'Arcangelo, E; Irace, A; Breglio, G; Spirito, P; “Experimental characterization of temperature distribution on power MOS devices during Unclamped Inductive Switching” MICROELECTRONICS RELIABILITY 2004 SEP-NOV VL 44 IS 9-11 Pp 1455 1459

[4] S. Grauby, S. Dilhaire, S. Jorez, W. Claeys, “Temperature Variation Mapping of a Microelectomechanical System by Thermoreflectance imaging” IEEE Electron Device Letters, Vol. 26, No. 2, Feb.2005.

[5] V. Quintard, S. Dilhaire, T. Phan, W. Claeys, “Temperature Measurements of Metal Lines Under Current Stress by high Resolution Laser Probing” IEEE Trans. on Instrumentation and Measurement VOL.48, N. 1, Feb. 1999.

[6] J. Christofferson, D. Vashaee, A. Shakouri “Thermoreflectance Imaging of Superlattice Micro Refrigerators”

[7] O. Breitenstein, M. Langenkamp "Lock-in Thermography" Springer 2003, ISBN 3-540-43439-9